Surface changes in the North Atlantic meridional overturning circulation during the last millennium

Alan D. Wanamaker Jr[1,2], Paul G. Butler[2], James D. Scourse[2], Jan Heinemeier[3], Jón Eiríksson[4,5], Karen Luise Knudsen[6] & Christopher A. Richardson[2]

Despite numerous investigations, the dynamical origins of the Medieval Climate Anomaly and the Little Ice Age remain uncertain. A major unresolved issue relating to internal climate dynamics is the mode and tempo of Atlantic meridional overturning circulation variability, and the significance of decadal-to-centennial scale changes in Atlantic meridional overturning circulation strength in regulating the climate of the last millennium. Here we use the time-constrained high-resolution local radiocarbon reservoir age offset derived from an absolutely dated annually resolved shell chronology spanning the past 1,350 years, to reconstruct changes in surface ocean circulation and climate. The water mass tracer data presented here from the North Icelandic shelf, combined with previously published data from the Arctic and subtropical Atlantic, show that surface Atlantic meridional overturning circulation dynamics likely amplified the relatively warm conditions during the Medieval Climate Anomaly and the relatively cool conditions during the Little Ice Age within the North Atlantic sector.

[1] Department of Geological and Atmospheric Sciences, Iowa State University, Ames, Iowa 50011–3212, USA. [2] School of Ocean Sciences, College of Natural Sciences, Bangor University, Menai Bridge, Anglesey, LL59 5AB, UK. [3] AMS [14]C Dating Centre, Department of Physics and Astronomy, Aarhus University, Ny Munkegade 120, DK-8000 Århus C, Denmark. [4] Earth Science Institute, University of Iceland, Askja, IS-101 Reykjavik, Iceland. [5] Centre for GeoGenetics, Natural History Museum of Denmark, University of Copenhagen, Øster Voldgade 5-7, DK-1350 Copenhagen, Denmark. [6] Department of Geoscience, Aarhus University, DK-8000 Århus C, Denmark. Correspondence and requests for materials should be addressed to A.D.W. (email: adw@iastate.edu).

Palaeoclimate records from sediments beneath the Florida Current indicate that the Gulf Stream transport decreased by ~10% during the Little Ice Age (LIA)[1]. It has been suggested that decreased meridional heat transport by the Gulf Stream and the North Atlantic Current (NAC) may have been partly responsible for LIA cooling[1–4]. Instrumental series of Gulf Stream/NAC and Atlantic meridional overturning circulation (AMOC) behaviour and heat transports are limited to a few decades[5]. Given this lack of long instrumental records, information about ocean variability in the North Atlantic on longer timescales can only be obtained from geological proxy archives.

To better understand the physical causes of the Medieval Climate Anomaly (MCA) and LIA climate intervals, additional high-quality palaeodata[6], from diverse geographic settings, including the global oceans, are required to confidently document the spatial and temporal scope of the MCA and LIA. Although the dynamical origins of the MCA and LIA have been widely studied[1,3,4,7–22], many aspects of these climate intervals are still poorly characterized and widely debated[4,7–9,11–17,21,22]. Key candidate forcings include external climate drivers (for example, volcanic and solar activity) and internal Earth system feedbacks. Beyond external climate forcings[12,20], it is recognized that natural variability in heat transport via the Gulf Stream and the NAC (which together make up the northward-flowing surface component of the AMOC) to higher latitudes within the Atlantic basin was likely influential in shaping the MCA and LIA climate events[1–4]. However, this hypothesis has been difficult to test because of a scarcity of suitable precisely dated natural marine proxy archives located within the region of influence of the AMOC.

To reconstruct the dynamics of Arctic and Atlantic water masses in this region over the last millennium, we analysed the radiocarbon content of samples obtained from shell growth increments of the long-lived marine bivalve *Arctica islandica*, which have been absolutely dated using crossdating techniques derived from dendrochronology[23]. The shells used in this study were collected from the North Icelandic shelf at 80 m water depth adjacent to the location of the modern oceanic Polar Front (Fig. 1), a region noted for its sensitivity to surface AMOC changes[24–26]. Because the shell chronology[27] is absolutely dated, ^{14}C values derived from known-age shell subsamples can be used to precisely constrain the relative ^{14}C age of water masses. Hence, the absolutely dated radiocarbon data presented here serve as a water mass tracer, rather than as a chronometer. To explore the differences between the global ocean (Marine09)[28,29] and the Icelandic shell-derived ^{14}C record, and to investigate potential causal mechanisms that link the shell ^{14}C record with North Atlantic Ocean circulation dynamics, we present our radiocarbon data in ΔR format. The ΔR values are determined by the regional deviations in the marine radiocarbon reservoir age from the modelled ocean surface mixed layer reservoir age (Marine09)[28–30]. To first order, ΔR reflects oceanic mixing processes (upwelling, advection) that contribute to the offset between regional and global ocean ^{14}C ages[30]; thus, ΔR time series can be used to trace water masses and ocean circulation. North of Iceland, relatively young Atlantic sourced waters (NAC) and relatively old Arctic sourced waters converge and mix (Fig. 1) in the vicinity of the oceanic Polar Front[24]. NAC waters (ΔR values = 0 to 50)[24] flow northward and clockwise around West Iceland as the Irminger Current and mix on the North Icelandic shelf with Arctic water (ΔR values > 150)[24,31,32], flowing southeastward as the East Icelandic Current (a periodic development of the East Greenland Current; Fig. 1)[33]. Our findings indicate a declining influence of NAC waters on the North Icelandic shelf during the last millennium. Since *circa* AD 1940, NAC-derived surface waters have again become more influential north of Iceland and within the Arctic[10], resembling hydrographic conditions present during the early MCA. We infer that the surface AMOC was relatively strong in Medieval times, became weaker in the LIA, and strengthened again after *circa* AD 1940. We suggest that the surface component of the AMOC amplified the relatively warm[13] conditions during the MCA and the relatively cool[13] conditions during the LIA within the North Atlantic Ocean.
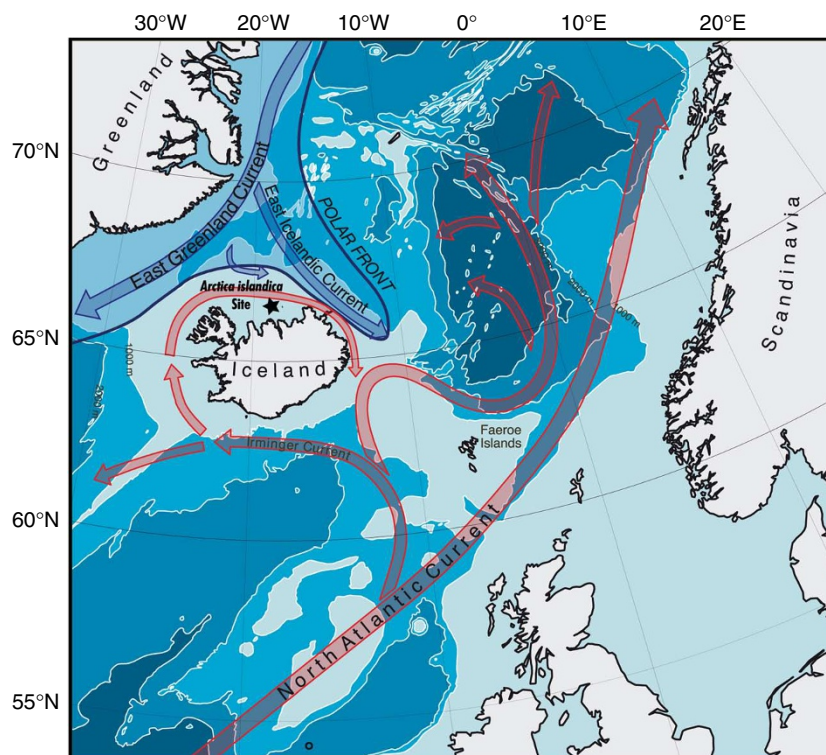

Figure 1 | Location map of modern ocean surface circulation patterns in the northern North Atlantic. The *A. islandica* study site on the North Icelandic shelf is shown with a star; map modified from ref. 25.
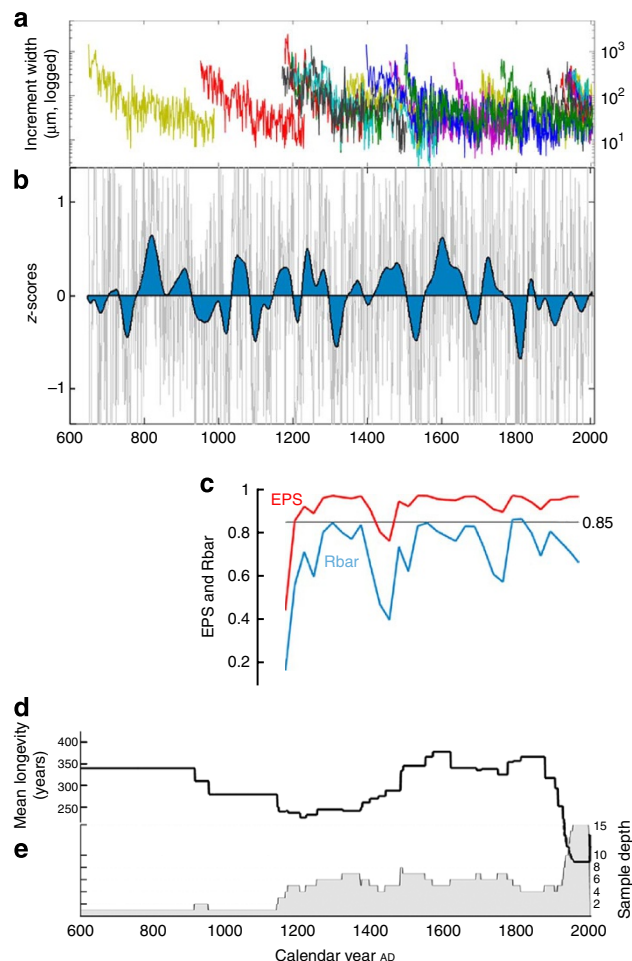
Figure 2 | Master shell chronology from the North Icelandic shelf and chronology statistics. (**a**) Raw increment widths (logged) for each of the 29 shells used in the master shell chronology. (**b**) Detrended growth increments normalized as *z*-scores ((value − mean)/standard deviation) derived from the autoregressive modelled chronology with a 70-year low pass centrally weighted Gaussian filter; see ref. 27 for additional details. (**c**) Expressed population signal (EPS; red) with the 0.85 critical value noted, and the mean correlation between all detrended series (Rbar; blue). (**d**) Mean longevity of all shells in the chronology at that point. (**e**) Sample depth of chronology at that point.

Results

Master shell chronology. A total of 29 shells (14 dead-collected and 15 live-collected) were used to construct the master shell chronology[27]. The shell chronology[27] extends 1,357 years, and represents the longest continuous annually resolved sclerochronological record (Fig. 2). The mean correlation between all detrended series (Rbar; blue line in Fig. 2c)[34] is defined only after *circa* AD 1200, because, before then, sample depth does not exceed two at any point (Fig. 2e). The value of Rbar (determined in a 50-year window at 25-year intervals) is low around AD 1200, probably because a prevalence of juvenile specimens in the chronology at that point introduces greater ontogenetic variability. It also falls slightly around AD 1450–1500 and in the late 1700s, indicating a weaker common signal. The Expressed Population Signal (EPS; red line in Fig. 2c)[35] takes account of both Rbar and the sample depth N (EPS = N×Rbar/(N×Rbar+ (1−Rbar))) to give an indication of the degree to which the population subsample, included in the chronology, expresses the theoretical population-wide common environmental signal. By convention, EPS ≥0.85 is taken to indicate that the expression of the common
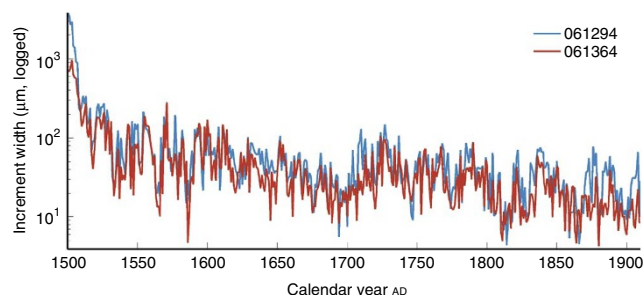

Figure 3 | Extreme longevity and centuries of synchronous shell growth. Raw increment width measurements (logged here to improve clarity) during a 410-year period (AD 1500–1909) for 2 very long-lived specimens of *A. islandica*, showing the strength of synchronous growth throughout ($r = 0.89$; $P < 0.0001$; $N = 410$).

signal is adequate[35]. Here the EPS falls below 0.85 only at the start of the period for which it is defined (*circa* AD 1200) and during the period AD 1450–1500, when the common signal is relatively weak. It is also notable that EPS does not increase significantly during the twentieth century when the inclusion of a number of live-collected specimens in the chronology raises the sample depth to 15. This indicates that for increment width series that correlate as closely as these, a sample depth between four and six is normally sufficient to provide an adequate signal to noise ratio. The longevity of the animals used here, determined by increment counting and cross-dating, ranks them among the longest lived non-colonial animals known to science. Of particular note are shells 061294 and 061364, which lived for 507 years and 412 years, respectively[27]. These two animals seem to have settled on the sea floor north of Iceland at about the same time (*circa* AD 1500), and the raw increment widths from their shells correlate strongly ($r = 0.89$; $P < 0.0001$) through a period of 410 years (Fig. 3).

Origin of radiocarbon signal in shells. To determine the likely origin of the radiocarbon signal (atmospheric versus oceanic) in the cross-dated shells, we compared the shell ^{14}C data with the radiocarbon record for the atmosphere (IntCal09)[28] and the modelled global ocean (Marine09)[28] (Fig. 4). During this interval (AD 600 to AD 1950), the modelled global ocean[28,29] is on average 386 (±39) years older than the atmosphere with respect to radiocarbon (Fig. 4; also see ref. 29, for a detailed discussion). Further, changes in the global ocean ^{14}C record are slightly lagged and attenuated compared with the atmosphere. In the early part of the record (AD 675 to AD 705 and AD 870 to AD 940) (highlighted as Case #1 in Fig. 4), the shell-derived ^{14}C values match the global ocean values. This indicates that a water mass of Atlantic origins (for example, NAC, a water mass that is about 400-years old with respect to radiocarbon) was prevalent on the North Icelandic shelf during the early MCA. Conversely, from AD 1000 to AD 1210, there was a clear departure in shell ^{14}C values from the global ocean (highlighted as Case #2 in Fig. 4) indicating relatively older waters on the North Icelandic shelf; these data are most consistent with a water mass of Arctic origins[24]. This apparent trend (increasing marine radiocarbon reservoir effect) continues into the LIA, until it is briefly interrupted by an atmospheric ^{14}C pulse from AD 1375 to AD 1400, which is clearly seen in the Marine09 record and the ^{14}C shell data (highlighted as Case #3 in Fig. 4). At least one other atmospheric ^{14}C perturbation is noted in the shell-based ^{14}C at ~AD 1790 (highlighted as Case #4 in Fig. 4). During the entirety of the LIA climate interval, waters along the North Icelandic shelf are older than the global ocean. For the first time since the early MCA, shell-based ^{14}C values equal the global ocean values at AD 1895 and AD 1950, likely indicating a shift to Atlantic-derived waters. Although decadal trends in
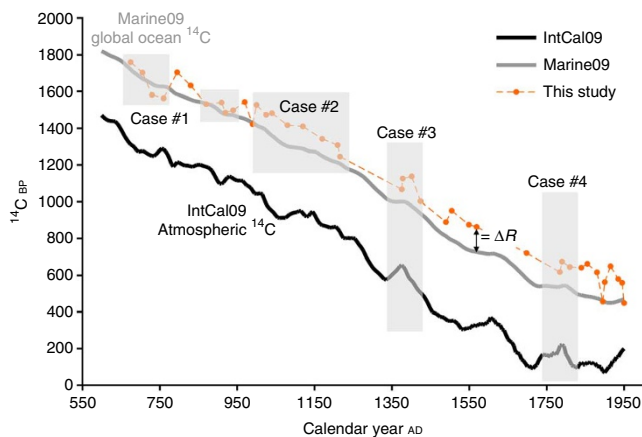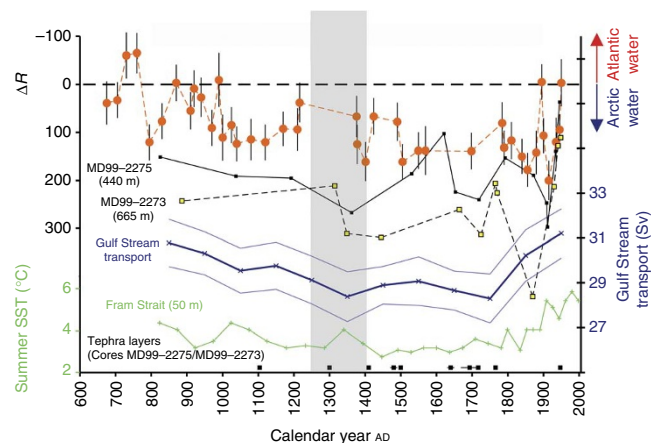
Figure 4 | Relationship between global and shell radiocarbon datasets. Cross-dated shell-based ^{14}C values (this study; solid orange circles) from known-age samples are compared with the atmospheric (IntCal09)[28] and the global ocean (Marine09)[28] radiocarbon records from AD 600 to AD 1950. In case #1 (early MCA), the shell ^{14}C record matches the modelled Marine09 (ref. 28) radiocarbon record (marine radiocarbon reservoir effect 386 ($\pm$39)[28,29]. In case #2, the shell ^{14}C record deviates from the Marine09 (ref. 28) record, indicating a relatively older (with respect to radiocarbon) water mass present on the North Icelandic shelf after AD 950. This long-term deviation between the shell-based and Marine09 radiocarbon records continues into the early twentieth century. Atmospheric ^{14}C pulses that are noted in the Marine09 and shell-based radiocarbon records are highlighted as case #3 and #4. An example of ΔR (ref. 30) (difference between shell ^{14}C age and the Marine09 ^{14}C age) is noted at ~AD 1560 for reference (see Fig. 5). BP = before present (BP = 0 at AD 1950).

**Figure 5 | Comparison of ΔR data with other AMOC-sensitive proxy records.** Shell-based ΔR values (this study; solid orange circles) and sediment-based ΔR values[24] (solid squares; MD99-2275 and MD99-2273) are compared with Gulf Stream transport estimates[1] (blue) in the Florida Straits and SST values from within the Arctic Ocean[10] (marine sediment record from Fram Strait off western Svalbard, 79°N; green) during the last millennium. More positive ΔR values are representative of Arctic-derived water masses, whereas less positive ΔR values are indicative of Atlantic-derived surface waters[24]. Relatively warmer SST values in Fram Strait indicate a strong Atlantic inflow to the Arctic, while relatively cool SST values likely represent a weak Atlantic inflow to the Arctic[10]. The errors in the Marine09 ^{14}C value[28] and the AMS ^{14}C measurement were propagated as random errors yielding a total ΔR_{shell} error. Tephra layers in marine sediment cores (MD99-2275 and MD99-2273) are shown along the bottom (solid black squares) to illustrate the age control for sediment sequences north of Iceland[24]. The age/depth models for the Fram Strait and Gulf Stream data are based on linear interpolation between calibrated AMS ^{14}C ages, and the Fram Strait data have an age error of about $\pm$30 to 50 years (see ref. 10 for the full SST record and details); the Gulf Stream data have a possible age error of about $\pm$50 years[1]. The horizontal grey bar represents the approximate regional timing of the MCA/LIA transition in the marine environment (that is, North Icelandic shelf) noted by refs 24–26.

atmospheric ^{14}C dynamics are faithfully recorded in the shell record (Fig. 4), the increasing deviation between the Marine09 record and the shell-based radiocarbon signal north of Iceland cannot be explained by atmospheric forcing.

Changes in ΔR data during the last millennium. We present 41 new ΔR_{shell} data (orange circles) spanning AD 675 to AD 1950; the subsamples necessarily integrate several annual increments, so some measurements have a temporal integration of 5 to 20 years (Fig. 5; Supplementary Data 1). The ΔR_{shell} values gradually increase over the last millennium, reflecting a shift towards older Arctic-derived water. Decadal- to multi-decadal scale variations in ΔR_{shell} values are most pronounced in the early part of the record and since *circa* AD 1800. Comparison with known present-day measurements of ΔR (ref. 36) indicates that ΔR_{shell} values before and during the early MCA[15] (for example, AD 675-AD 1000) mostly reflect waters derived from an Atlantic (NAC) source, whereas during much of the MCA[15] (after AD 1000) and into the early LIA[24] they indicate a varying mixture of Atlantic and Arctic sources. Progressing into the LIA (after AD 1500), the ΔR_{shell} values are most consistent with a dominant Arctic (East Icelandic Current) source. In AD 1915, the highest ΔR_{shell} value ($\Delta R = 200$) is reached. After AD 1915, there is an apparent reversal in ΔR_{shell} values.

Comparison of ΔR data with other AMOC-sensitive proxy records. To establish a more comprehensive reconstruction of ΔR variability along the North Icelandic shelf, we compare our results with sediment-based ΔR values from two high-resolution records[24] (squares) collected from the vicinity of the shell location, but at 440 m (core MD99-2275) and 665 m (core MD99-2273) water depths, respectively (Fig. 5). Because of the positions of these sediment archives, numerous Holocene tephras from Icelandic volcanic

sources[37] are available to constrain their age/depth relationship[24] (bottom Fig. 5). These records indicate an increase in ΔR values during the last millennium (Fig. 5) consistent with the shell values, but a depth-dependent relationship with ΔR is also apparent. The relationship between water depth and ΔR can be explained by the greater contribution of relatively depleted ^{14}C water that penetrates onto the shelf at greater depths[24]. All three records show a long-term trend to increasing ΔR values before *circa* AD 1880, reflecting reduced influence of NAC-derived waters. However, the ΔR data show a large degree of variability after AD 1880, likely indicating increased variability of oceanographic conditions on the North Icelandic shelf. After *circa* AD 1940, ΔR decreases rapidly towards levels characteristic of the early MCA, suggesting a renewed influence of Atlantic sourced waters on the North Icelandic shelf.

Role of upwelling on the ΔR record. Although regional upwelling can complicate the interpretation of ΔR, the lack of any covariance ($r^2 = 0.01$) between co-registered shell carbon isotope ($\delta^{13}C$) and ^{14}C measurements (converted to ΔR values) (Fig. 6; Supplementary Data 1), both of which are sensitive proxies of upwelling[38], strongly indicates that upwelling is not a control on the Icelandic ΔR values.

Discussion

Even though we are arguing that the long-term trend in ΔR_{shell} values reflects water mass variability, it is possible to make an alternative
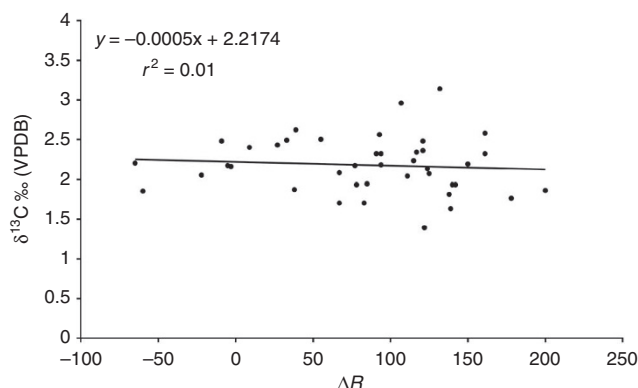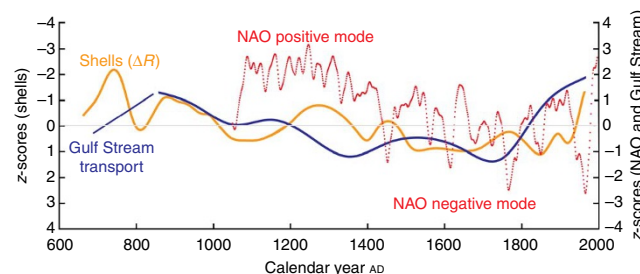
Figure 6 | Relationship between shell-stable carbon isotope ratios and radiocarbon values. Linear fit and regression statistics for the relationship between co-registered $\delta^{13}C$ and ^{14}C shell samples (shown here as ΔR values).

Figure 7 | Relationship between winter NAO and shell ΔR values. z-scores of shell-based ΔR values (this study; orange) and Gulf Stream transport estimates (ref. 1) (blue) are compared with the raw data used in the wintertime NAO reconstruction (ref. 14) (red). Shell ΔR values and Gulf Stream transport data were fit with a smoothing spline function (p parameter = 0.0003) to highlight the low frequency evolution and coherence of these series.

case that it results from atmospheric ^{14}C dynamics. By definition, regional ΔR values are derived by subtracting the modelled global ocean ^{14}C value from the measured $^{14}C_{shell}$ value for a given calendar year (in this case, the sclerochronologically determined year) as noted above[30]. The global ocean ^{14}C value is determined by modelling the atmospheric ^{14}C record (INTCAL09; see ref. 28), which is based on the ^{14}C content of cross-dated tree-ring records. The model used to assign global ocean ^{14}C values is based on a simple gas exchange model (for more details see ref. 30). As defined by ref. 30, the ΔR value is composed of two terms: the portion of the shift in regional marine ^{14}C age attributable to a regional atmospheric ^{14}C age difference, and an additional shift in marine regional ^{14}C age, which reflects oceanic processes (such as upwelling and/or advection) that differ from the parameters in the simulated global ocean. Although rapid, decadal-scale atmospheric perturbations in ^{14}C production seem to impact the ΔR record (Fig. 4, Cases #3 and #4), gradual and largely unidirectional changes in ^{14}C activity in the atmosphere (as noted in INTCAL09 for this interval AD 650 to AD 1950; Fig. 4) will not impact the ΔR values, because these changes are also embedded in the Marine09 model, albeit with a slight lag. Because the ^{14}C Marine09 data are a smoothed version (with appropriate lag times) of the ^{14}C atmospheric data (for example, INTCAL09), the increasing deviation in ΔR during the last millennium at the study site must be of oceanic origin. Hence, we argue that the ΔR values north of Iceland primarily reflect processes indicative of large-scale ocean circulation dynamics.

The proxy transport estimates from the Florida Straits[1] capture a large portion of the northward flow of the Gulf Stream/NAC system (Fig. 5). Comparison of these data with the ΔR values from the North Icelandic shelf suggests that the latter are coupled to Gulf Stream/NAC discharge and the wind-driven (surface) component of AMOC. The associated distinct and converging water masses (Atlantic and Arctic) associated with the oceanic Polar Front (Fig. 1) are largely driven by regional wintertime mean sea-level pressure gradients[39] and wind-stress curl over the region[40]. Hence, changes in regional and basin-scale surface wind patterns, such as the North Atlantic Oscillation (NAO), will in part modulate the flux of Atlantic waters flowing northward to Iceland via the Irminger Current[40].

Over the last millennium, the winter NAO system has been variable, with a strongly positive NAO mode during Medieval times and a neutral to slightly negative NAO mode during the LIA[14]. Over recent decades, the NAO system has been in strong positive mode, similar to the MCA[14]. We hypothesize that the variability in surface AMOC and ΔR values north of Iceland are in part driven by the mean state of the NAO system during the last 1,000 years

(Fig. 7). The northerly position of the Gulf Stream wall, Gulf Stream transport, and surface AMOC dynamics are positively correlated with winter NAO values[41–45]. Additionally, model results link a strengthened AMOC with a northward shift of the path of the Gulf Stream[45]. Under such conditions, a relatively enhanced transport of Atlantic water is carried northwards as the NAC, ultimately decreasing ΔR values north of Iceland. We infer that the surface component of the AMOC was relatively strong in early Medieval times, became weaker in the LIA, and stronger again after AD ~1940. This inference is corroborated by recent summer sea surface temperature (SST) proxy-based estimates from within the Arctic Ocean[10] (Fram Strait off western Svalbard; 79°N), a region that is also sensitive to surface AMOC dynamics. The Fram Strait SST data[10] indicate that the flux of Atlantic water entering the Arctic Ocean has substantially increased in the last 100 to 200 years (Fig. 5), likely causing a significant portion of the modern Arctic warming[10]. Additionally, the relative strength of Atlantic inflow (and associated heat transport) to Fram Strait was apparently high during the MCA and low during the LIA[10] (Fig. 5). The long-term covariance between Gulf Stream transport estimates and the relative influence of Atlantic and Arctic waters on the North Icelandic shelf (Fig. 5) support the conclusion that the surface strength of the AMOC primarily controls ΔR values north of Iceland. Additionally, sediment-based SST data[24–26] from the North Icelandic shelf and Fram Strait[10] indicate a relatively warm MCA and cold LIA synchronous with the ΔR data and the evolution of Gulf Stream transport.

Although certain mechanistic and dynamical models link aspects of AMOC behaviour to winter NAO forcing[43], considerable uncertainty remains regarding the physical mechanisms driving this variability at the decadal- to centennial-scale[46]. The current lack of adequately resolved and well-distributed marine proxy data for the strength of AMOC over the last millennium prevents a rigorous testing of the main factors that modulate surface AMOC variability. Additional work is required to establish the boundary conditions and possible mechanisms (for example, increased volcanism in the thirteenth century[20] and changing Arctic sea ice conditions[47,48]) that led to the inferred surface AMOC weakening and general cooling trend into the LIA climate interval. Despite some progress noted here in documenting the past behaviour of the surface AMOC variability, this study does not reveal any information regarding deep-water formation (rates or volumes) related to AMOC in the northern North Atlantic during this interval. Hence, our understanding of links between the overturning circulation (specifically deepwater formation) and North Atlantic climate, during the last millennium, remains incomplete. The acquisition of high-resolution marine proxy data from regions sensitive to AMOC changes (both surface and deepwater processes) is therefore a major research priority.

Methods

Shell collection. The shells used in this study were part of a collection of live, dead articulated, and dead single valves of *A. islandica* collected by trawling the seabed surface with a bespoke dredge on the North Icelandic shelf (Fig. 1) in June 2006 from the RV *Bjarni Sæmundsson* (Cruise No. B05-2006). Shells were collected near the island of Grimsey (66° 31.59′ N, 18° 11.74′ W) at a water depth of 81–83 m (trawl B05AD03)[49].

Radiocarbon analysis. To identify shells from long-lived animals that had been alive during the target period and that might therefore be used in an absolutely dated chronology, 24 of the largest and heaviest of the dead-collected shells were initially selected for AMS radiocarbon dating. The periostracum was removed by scraping the outer shell surface using a razor blade near the targeted region and an ~10–30 mg solid sample of shell carbonate was cut and removed from the outer shell surface for radiocarbon sampling. The shell samples were treated following a standard mollusc-rinsing procedure at Aarhus University AMS [14]C Dating Centre (Denmark); to eliminate any possible surface contamination, the outer 25% of the shell was removed by etching in 1 M HCl. Any organic carbon incorporated in the shell carbonate was removed by treatment with a $KMnO_4$ solution for 16–20 h at 80 °C. The CO_2 was liberated with ~100% phosphoric acid in an evacuated vial at 25 °C. Part of the CO_2 was used for $\delta^{13}C$ measurements; the remainder was converted to graphite for AMS ^{14}C measurements on the Centre's EN tandem accelerator by reduction with H_2, with cobalt as a catalyst.

Shell chronology. Additional detailed methods regarding the construction of the master shell chronology are outlined in ref. 27. In brief, the shell valves were sectioned along the axis of maximum growth from the hinge tooth at the umbo to the outer shell margin. The exposed surface was ground and polished, then etched in one of two ways: either in a modified Mutvei solution[49,50] or in 0.1 M HCl for 2 to 4 min (ref. 51). An acetate peel replica was taken of the etched surface from which the annual growth increments could be viewed under transmitted light and measured using dedicated software (see ref. 49 for additional details). Of the 24 dead-collected shells that were radiocarbon dated, 6 were dated before the target period and a further 4 could not be reliably measured because their increments could not be visualized with sufficient resolution. The other 14 were measured and cross-dated and, in all cases, their sclerochronologically determined calendar ages were found to be consistent with their calibrated radiocarbon ages. Growth in *A. islandica* is similar to growth in trees in that it is characterized by strong ontogenetic trends in increment width and variance[23]. These trends can be removed with the same detrending techniques that are used in dendrochronology. For crossdating, the measured growth increment series were high-bandpass-filtered by taking residuals from a 15-year spline applied to the logarithms of the increment widths[51]. For chronology construction, lower frequency variability was preserved by taking residuals from a negative exponential function applied to a data adaptive power transformation of the raw increment width series[52]. The dendrochronology software ARSTAN was used to construct the chronology as an autoregressively modelled biweight robust mean function of the detrended increment width series (ARSTAN for WINDOWS 41d; ref. 53). Sample depth is at least 4 after AD 1194. The shell record has been extended to AD 649 with the addition of two index series (shell 061312 and shell 061664). Shell 061312 correlates significantly with the chronology (mean value of 4 series excluding 061312), during AD 1200–31 ($r = 0.69$; $N = 32$; $P < 0.001$), and shell 061664 correlates significantly with 061312 during AD 952-88 ($r = 0.61$; $N = 37$; $P < 0.001$). Pending the identification of coeval shells that can be used to increase the sample depth and strengthen the dating model during this period, absolute dating earlier than AD 1194 cannot be guaranteed. The master shell chronology is cross-dated (minimum replication of 4 shells) from AD 1194 to AD 2005. The mean longevity of the shells in the chronology generally exceeds 200 years (Fig. 2d), dropping only after AD 1934 when several live-collected shells enter the chronology. Eight of the shells used in the chronology are from animals, which lived for more than 300 years.

Calculation of ΔR. To determine the deviation in the local marine radiocarbon reservoir age (ΔR) north of Iceland, the modelled ocean (via Marine09; see ref. 28) ^{14}C value, for the sclerochronologically determined calendar year of the sample, was subtracted from the ^{14}C shell value determined by AMS dating (see ref. 30 and Supplementary Data 1).

Updated ΔR values for shells 061294 and 061315. The individual specimen (shell 061294) reported here as having lived for 507 years has previously been reported with a lifetime of 405-to-410 years[49]. This adjustment was a consequence of a refinement in the method of increment counting[27]. Previously, when working with shells from UK waters with lifetimes of up to 250 years, measurement in the hinge-plate region was recommended[51], because the increments there were less vulnerable to the disturbance caused by external shocks and were generally easier to visualize. *A. islandica* from the North Icelandic shelf, however, are more long-lived than those from UK waters[23,27,51] and are also slightly smaller. In these shells, the smaller increments in the hinge plate can be so tightly packed that they can no longer be distinguished, and it is possible for groups of narrow increments to be counted as a single increment. Subsequent to the initial report of the longevity
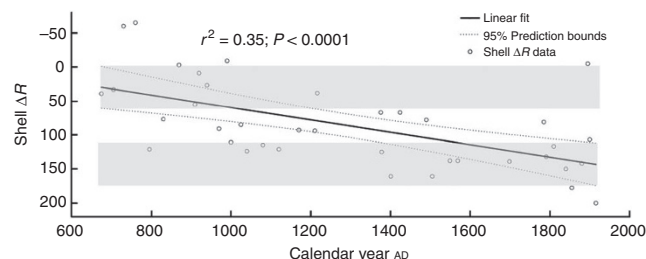
Figure 8 | Millennial-scale trend in shell ΔR values. Linear fit and regression statistics of the shell ΔR data (AD 675 to AD 1915) are shown. The data were modelled (solid black line) using MatLab (version R2010A; Curve Fitting Toolbox) to establish the uncertainty in modelled shell ΔR data. The 95% (confidence interval) prediction bounds (dashed lines) of the model are shown, and these results illustrate that the prediction bounds do not overlap between the early and late parts of the record (highlighted rectangles).

of shell 061294, it was remeasured on the outer shell margin and cross-dated (Fig. 3) with other contemporary specimens, thus confirming the redetermined longevity, and highlighting the utility of crossdating and emphasizing the high level of synchronous growth in *A. islandica* populations. The ΔR values reported here for shells 061294 and 061315 reflect the adjustments of the sclerochronological years of the samples taken for radiocarbon analysis, and the ΔR values for shells 061294 and 061315, reported by ref. 49, are superseded by values reported here (Supplementary Data 1).

Statistical evaluation of the millennial-scale ΔR_shell trend. To test whether the ΔR_{shell} trend is statistically significant before the modern ΔR_{shell} transition (Fig. 5), we fit the data (AD 675 to AD 1915) with a simple linear regression model (Fig. 8). On the basis of the regression statistics ($r^2 = 0.35$; $P < 0.0001$) and the fact that the model results (95% confidence interval; Curve Fitting Toolbox in MatLab R2010A) do not overlap (shown by the highlighted rectangles) in the early and late parts of the record, we conclude that the ΔR_{shell} trend during the last millennium is robust and statistically valid. We only modelled data from AD 675 to AD 1915, because the most positive ΔR values in the shells and sediments occurred around AD 1915.

References

1. Lund, D. C., Lynch-Stieglitz, J. & Curry, W. B. Gulf Stream density structure and transport during the past millennium. *Nature* **444,** 601–604 (2006).
2. Lynch-Stieglitz, J., Curry, W. B. & Lund, D. C. Florida Straits density structure and transport over the last 8000 years. *Paleoceanography* **24,** 1–9 (2009). doi:10.1029/2008pa001717.
3. Denton, G. H. & Broecker, W. S. Wobbly ocean conveyor circulation during the Holocene? *Quaternary Sci. Rev.* **27,** 1939–1950 (2008).
4. Trouet, V., Scourse, J. D. & Raible, C. C. North Atlantic storminess and Atlantic meridional overturning circulation during the last millennium: reconciling contradictory proxy records of NAO variability. *Global Planet. Change* **84–85,** 48–55 (2012).
5. Bryden, H. L. *et al.* Slowing of the Atlantic meridional overturning circulation at 25°N. *Nature* **438,** 655–657 (2005).
6. Jones, P. D. *et al.* High-resolution palaeoclimatology of the last millennium: a review of current status and future prospects. *Holocene* **19,** 3–49 (2009).
7. Jones, P. D. & Mann, M. E. Climate over past millennia. *Rev. Geophys.* **42,** 1–42 (2004), doi:10.1029/2003rg000143.
8. Matthews, J. A. & Briffa, K. R. The 'Little Ice Age': re-evaluation of an evolving concept. *Geogr Ann A* **87A,** 17–36 (2005).
9. Bradley, R. S., Hughes, M. K. & Diaz, H. F. Climate in Medieval time. *Science* **302,** 404–405 (2003).
10. Spielhagen, R. F. *et al.* Enhanced modern heat transfer to the Arctic by warm Atlantic water. *Science* **331,** 450–453 (2011).
11. Broecker, W. S. Was a change in thermohaline circulation responsible for the Little Ice Age? *Proc. Natl Acad. Sci. USA* **97,** 1339–1342 (2000).
12. Crowley, T. J. Causes of climate change over the past 1000 years. *Science* **289,** 270–277 (2000).
13. Mann, M. E. *et al.* Global signatures and dynamical origins of the Little Ice Age and medieval climate anomaly. *Science* **326,** 1256–1260 (2009).
14. Trouet, V. *et al.* Persistent positive North Atlantic oscillation mode dominated the Medieval climate anomaly. *Science* **324,** 78–80 (2009).
15. Graham, N., Ammann, C., Fleitmann, D., Cobb, K. & Luterbacher, J. Support for global climate reorganization during the 'Medieval Climate Anomaly'. *Climate Dynam.* **37,** 1217–1245 (2011), doi:10.1007/s00382-010-0914-z.

16. Palastanga, V. *et al.* Atmosphere and ocean dynamics: contributors to the European Little Ice Age? *Climate Dynam.* **36,** 973–987 (2010).

17. Diaz, H. F. *et al.* Spatial and temporal characteristics of climate in Medieval times revisited. *B. Am. Meteorol. Soc.* **92,** 1487–1500 (2011).

18. Keigwin, L. D. The Little Ice Age and Medieval Warm Period in the Sargasso sea. *Science* **274,** 1503–1508 (1996).

19. Kreutz, K. J. *et al.* Bipolar changes in atmospheric circulation during the Little Ice Age. *Science* **277,** 1294–1296 (1997).

20. Miller, G. H. *et al.* Abrupt onset of the Little Ice Age triggered by volcanism and sustained by sea-ice/ocean feedbacks. *Geophys. Res. Lett.* **39,** L02708 (2012).

21. Hughes, M. K. & Diaz, H. F. Was there a 'Medieval Warm Period', and if so, where and when? *Climatic Change* **26,** 109–142 (1994).

22. Crowley, T. J. & Lowery, T. S. How warm was the Medieval Warm Period? *Ambio* **29,** 51–54 (2000).

23. Butler, P. G. *et al.* Continuous marine radiocarbon reservoir calibration and the ^{13}C Suess effect in the Irish Sea: Results from the first multi-centennial shell-based marine master chronology. *Earth Planet Sci. Lett.* **279,** 230–241 (2009).

24. Eiríksson, J. *et al.* Coupling of palaeoceanographic shifts and changes in marine reservoir ages off North Iceland through the last millennium. *Palaeogeogr. Palaeoclimat. Palaeoecol.* **302,** 95–108 (2011).

25. Ran, L., Jiang, H., Knudsen, K. L. & Eiríkson, J. Diatom-based reconstruction of paleoceanographic changes on the North Icelandic shelf during the last millennium. *Palaeogeogr. Palaeoclimat. Palaeoecol.* **302,** 109–119 (2011).

26. Sicre, M. A. *et al.* Sea surface temperature variability in the subpolar Atlantic over the last two millennia. *Paleoceanography* **26,** PA4218 (2011).

27. Butler, P. G. *et al.* Variability of marine climate on the North Icelandic Shelf in a 1,357-year proxy archive based on growth increments in the bivalve *Arctica islandica*. *Palaeogeogr. Palaeoclimat. Palaeoecol.* (2012), doi: 10.1016/j.palaeo.2012.01.016.

28. Reimer, P. J. *et al.* Intcal09 and Marine09 radiocarbon age calibration curves, 0–50,000 years Cal Bp. *Radiocarbon* **51,** 1111–1150 (2009).

29. Hughen, K. A. *et al.* Marine04 marine radiocarbon age calibration, 0–26 cal kyr BP. *Radiocarbon* **46,** 1059–1086 (2004).

30. Stuiver, M. & Braziunas, T. F. Modeling atmospheric C-14 influences and C-14 ages of marine samples to 10,000 BC. *Radiocarbon* **35,** 137–189 (1993).

31. Tauber, H. & Funder, S. ^{14}C content of recent molluscs from Scoresby Sund, central East Greenland. *Grønlands Geologiske Undersøgelese, Rapport* **75,** 95–99 (1975).

32. Hjort, C. A sea correction for East Greenland. *Geol. Foeren. Stockholm Foerh.* **95,** 132–134 (1973).

33. Hansen, B. & Osterhus, S. North Atlantic-Nordic Seas exchanges. *Prog. Oceanogr.* **45,** 109–208 (2000).

34. Briffa, K. & Jones, P. D. in *Methods of Dendrochronology: Applications in the Environmental Sciences* (eds Cook, E. R., Kairiukstis, L. A). 137–152 Kluwer Academic Publishers, Dordrecht, 1990).

35. Wigley, T. M. L., Briffa, K. R. & Jones, P. D. On the average value of correlated time series, with applications in dendroclimatology and hydrometeorology. *J. Clim. Appl. Meteorol.* **23,** 201–213 (1984).

36. Hakansson, S. University of Lund radiocarbon dates.16. *Radiocarbon* **25,** 875–891 (1983).

37. Larsen, G., Eiríksson, J., Knudsen, K. L. & Heinemeier, J. Correlation of late Holocene terrestrial and marine tephra markers, North Iceland: implications for reservoir age changes. *Polar Res.* **21,** 283–290 (2002).

38. Druffel, E. R. M. & Griffin, S. Large variations of surface ocean radiocarbon - evidence of circulation changes in the Southwestern Pacific. *J. Geophys. Res. Oceans.* **98,** 20249–20259 (1993).

39. Blindheim, J. & Malmberg, S. A. *The Mean Sea Level Pressure Gradient across the Denmark Strait as an Indicator of Conditions in the North Icelandic Irminger Current* 65–71 (American Geophysical Union, 2002).

40. Malmberg, S. A. & Kristmannsson, S. S. Hydrographic conditions in Icelandic waters, 1980–1989. *Hydrobiological Variability in the ICES Area, 1980–1989* **195,** 76–92 (1992).

41. Taylor, A. H. & Stephens, J. A. The North Atlantic oscillation and the latitude of the Gulf Stream. *Tellus* **50,** 134–142 (1998).

42. Joyce, T. M., Deser, C. & Spall, M. A. The relation between decadal variability of subtropical mode water and the North Atlantic Oscillation. *J. Climate* **13,** 2550–2569 (2000).

43. Curry, R. G. & McCartney, M. S. Ocean gyre changes associated with the North Atlantic Oscillation. *J. Phys. Oceanogr.* **31,** 3374–3400 (2001).

44. Bentsen, M., Drange, H., Furevik, T. & Zhou, T. Simulated variability of the Atlantic meridional overturning circulation. *Climate Dynam.* **22,** 701–720 (2004).

45. De Coetlogon, G. *et al.* Gulf Stream variability in five oceanic general circulation models. *J. Phys. Oceanogr.* **36,** 2119–2135 (2006).

46. Wunsch, C. & Heimbach, P. Estimated decadal changes in the North Atlantic meridional overturning circulation and heat flux 1993–2004. *J. Phys. Oceanogr.* **36,** 2012–2024 (2006).

47. Masse, G. *et al.* Abrupt climate changes for Iceland during the last millennium: evidence from high resolution sea ice reconstructions. *Earth Planet Sci. Lett.* **269,** 564–568 (2008).

48. Andrews, J. T., Belt, S. T., Olafsdottir, S., Masse, G. & Vare, L. L. Sea ice and marine climate variability for NW Iceland/Denmark Strait over the last 2000 cal. yr BP. *Holocene* **19,** 775–784 (2009).

49. Wanamaker, A. D. *et al.* Very long-lived mollusks confirm 17th century AD tephra-based radiocarbon reservoir ages for North Icelandic shelf waters. *Radiocarbon* **50,** 399–412 (2008).

50. Schöne, B. R., Dunca, E., Fiebig, J. & Pfeiffer, M. Mutvei's solution: an ideal agent for resolving microgrowth structures of biogenic carbonates. *Palaeogeogr. Palaeoclimat. Palaeoecol.* **228,** 149–166 (2005).

51. Scourse, J. *et al.* First cross-matched floating chronology from the marine fossil record: data from growth lines of the long-lived bivalve mollusc *Arctica islandica*. *Holocene* **16,** 967–974 (2006).

52. Cook, E. R. & Peters, K. Calculating unbiased tree-ring indices for the study of climatic and environmental change. *Holocene* **7,** 361–370 (1997).

53. Cook, E. R. & Krusic, P. J. *ARSTAN - A Tree-Ring Standardization Program Based on Detrending and Autoregressive Time Series Modeling, with Interactive Graphics* (Tree-Ring Laboratory, Lamont Doherty Earth Observatory of Columbia University, Palisade, NY, 2007).

Acknowledgements

Author contributions

J.D.S. and C.A.R. conceived the study. P.G.B. and A.D.W. led the development of the master shell chronology. A.D.W. is mainly responsible for sampling the shells for radiocarbon analysis, data interpretation, and led the writing of the paper. J.H. conducted the radiocarbon measurements. J.E. and K.L.K. contributed expertise on oceanography. J.D.S., P.G.B., J.H. and J.E. conducted fieldwork. All authors contributed to data interpretation and writing of the manuscript.

Additional information

Supplementary Information accompanies this paper at http://www.nature.com/naturecommunications

Competing financial interests: The authors declare no competing financial interests.

Reprints and permission information is available online at http://npg.nature.com/reprintsandpermissions/

How to cite this article: Wanamaker, A. D. *et al.* Surface changes in the North Atlantic meridional overturning circulation during the last millennium. *Nat. Commun.* 3:899 doi: 10.1038/ncomms1901 (2012).